ELSEVIER

Chemical Geology 201 (2003) 91–101

CHEMICAL GEOLOGY
INCLUDING
ISOTOPE GEOSCIENCE

www.elsevier.com/locate/chemgeo

The influence of dissolved humic acids on the kinetics of calcite precipitation from seawater solutions

Pierpaolo Zuddas*, Katavut Pachana, Damien Faivre

Laboratoire de Géochimie des Eaux, Institut de Physique du Globe, Université Denis Diderot 2, place Jussieu, F75254 Paris cedex 05, France

Received 26 February 2003; accepted 4 July 2003

Abstract

The influence of dissolved organic matter on the complex mechanism of calcite crystal growth from seawater was evaluated by a set of experiments at different humic acid concentrations (i.e. [HA] = 50, 500, 1000 μg/kg) in NaCl–$CaCl_2$ solutions at a total ionic strength of 0.7 mol/kg. The temperature and P_{CO_2} of the experiments were maintained at 298 K and 40 Pa, respectively. The constant addition technique was used in order to maintain $[Ca^{2+}]$ at ≅ 10.5 mmol/kg, while the $[CO_3^{2-}]$ was varied to isolate its role on the precipitation rate. Assuming that the calcite precipitation in this solution is dominated by the reaction:

$$Ca^{2+} + CO_3^{2-} \underset{k_b}{\overset{k_f}{\leftrightarrow}} CaCO_3 \quad (A1)$$

where k_f and k_b are the forward and reverse reaction rate constants, respectively, the net precipitation rate, R, can be described at any dissolved organic matter content by the difference between the forward and reverse rates:

$$R = k_f (a_{Ca^{2+}})^{n_1} (a_{CO_3^{2-}})^{n_2} - k_b \quad (A2)$$

or, in its logarithmic form:

$$\log(R + k_b) - \log K_f + n_2 \log[CO_3^{2-}] \quad (A3)$$

where n_i are the partial reaction orders with respect to the participating ions, a and γ are the ion activities and activity coefficients, respectively, and, $K_f = k_f (a_{Ca^{2+}})^{n_1} (\gamma_{CO_3^{2-}})^{n_2}$, a constant.

Results of this study indicate that, similarly to seawater and NaCl–$CaCl_2$ solutions at the same ionic strength, the partial reaction order with respect to the carbonate ion concentration is 3, while the forward reaction rate constant, K_f, decreases by one order of magnitude when the dissolved organic matter concentration increased from 0 to 1000 μg/kg. This suggests that the mechanism of calcite precipitation is independent of the dissolved organic matter concentration even if such a component inhibits the calcite precipitation rate. Applying our model to previous rate measurements carried out in seawater solution under the compositional condition $[Ca^{2+}] \gg [CO_3^{2-}]$, we found that the rate of calcite precipitation from seawater solutions, a complex function of P_{CO_2} and seawater inorganic inhibitors, still decreases as a function of the [HA] by at least one order of magnitude. Finally, we propose that the dissolved organic matter under the form of HA

* Corresponding author. Present address: Laboratoire de PaléoEnvironnement et PaléoBiosphère, Université Claude Bernard Lyon 1, Campus de la Doua 2, rue Dubois, F69622 Villeurbanne Cedex, France.

E-mail address: pierpaolo.zuddas@univ-lyon1.fr (P. Zuddas).

0009-2541/$ - see front matter © 2003 Published by Elsevier B.V.
doi:10.1016/S0009-2541(03)00230-4

inhibits the calcite precipitation rate from seawater by covering the active growth sites rather than by complexation of calcium in solution.
© 2003 Published by Elsevier B.V.

Keywords: Kinetics; Calcite crystal growth; Organic matter; Seawater

1. Introduction

Identification of the role played by organic compounds on the rate of carbonate precipitation has been the object of considerable effort, since it has been long suspected that organic coating on carbonate particles may, to some extent, explain the supersaturation of surface seawater with respect to calcium carbonate. Kitano and Hood (1965), Kitano and Kanamori (1966), Suess (1970) and Wada et al. (1993) indicate that the inhibition power of organic material present in seawater on calcite precipitation rate is roughly proportional to the association constant of the organic compounds with Ca^{2+}. They suggested that the inhibition can be related to calcium complex formation with strong and moderate organic ligands (i.e. citrate, malate, glycine and glycoprotein) that reduces the amount of free-Ca and decreases the saturation state of the solution with respect to $CaCO_3$. A similar hypothesis was postulated in the case of aragonite precipitation inhibition from seawater when dissolved organic matter was mainly constituted by humic substances and/or aromatic substances (Chave and Suess, 1970; Berner et al., 1978; Morse and Mackenzie, 1990). In particular, Berner et al. (1978) found that rates decreased by a factor of 50 in the presence of organic acids (i.e. gallic acid, mellitic acid, tannic acid, and fulvic and humic acids), although some compounds demonstrated little or no inhibition (i.e. amino acids and fatty acids). Bischoff (1968) found that acidic amino acids inhibited aragonite–calcite transformation rates, whereas 'neutral' amino acids catalysed this reaction.

Several rate equations have been proposed to describe the precipitation and/or dissolution kinetics of calcite under restricted sets of solution conditions. Berner and Morse (1974) recognised that a simple disequilibrium functionality could not satisfactorily explain the kinetics of calcite dissolution over a large pH range in seawater solutions and suggested that different reactions dominate over various pH ranges. Alternatively, a model which combines expressions for four elementary reactions (Plummer et al., 1978) was proposed to describe the rate of calcite dissolution in dilute solutions over a wide range of pH and P_{CO_2} values in terms of the sum of forward and reverse reaction rates. In more complex solutions like seawater, empirical expressions (Morse, 1978; Mucci, 1986; Burton and Walter, 1987) or mechanistic formulations (Zhong and Mucci, 1993; Zuddas and Mucci, 1994, 1998) have been adopted to describe the rates of calcite precipitation and dissolution. In these studies, it was demonstrated that a similar rate expression can be used to describe the kinetics of calcite precipitation in both seawater and $NaCl–CaCl_2$ solutions at the same ionic strength (i.e. 0.7 m) and calcium concentration and that an increase of the total ionic strength catalyses the calcite precipitation reaction.

The aim of this work was to evaluate the role of dissolved humic acid, HA, on the mechanism of calcite crystal growth from seawater. We also investigated the kinetics of this reaction in a simple, strong electrolyte solution, where the influence of major seawater constituents and known reaction inhibitors such as Mg^{2+} and SO_4^{2-} was neglected. The influence of HA, a 'minor' seawater constituent, on the rate and mechanism of calcite crystal growth was thus investigated in $NaCl–CaCl_2$ solutions at ionic strengths similar to seawater (i.e. 0.7 mol/kg) and maximum [HA] of 1 mg/kg.

2. A simplified theoretical view

The reaction of calcite crystal growth from strong electrolyte solutions like seawater is macroscopically represented by the addition of calcium and carbonate ions at the crystal surface. The role played by the surface during calcite crystal growth in the presence of dissolved HA can be described assuming that both HA and CO_3 molecules occupy neighbouring sites and that, the positive charged surface is covered by unoc-

cupied calcium, $>Ca^{2+}$ (Cicerone et al., 1992; Zuddas and Mucci, 1998). Let ϑ_{HA} and ϑ_{CO_3} be the fraction of the surface sites covered by HA and CO_3, respectively, and let ϑ_v be the fraction of sites that are vacant:

$$\vartheta_v = 1 - \vartheta_{HA} - \vartheta_{CO_3}. \quad (1)$$

The rate per unit area, v, is proportional to the fraction of surface sites (Castellan, 1983):

$$v = k \times > [Ca]^2 \times \vartheta_{HA} \times \vartheta_{CO_3} \quad (2)$$

As CO_3 and HA are attached to the surface, $CaCO_3$ and HACa molecule are adsorbed to the surface. Under such a condition, the two adsorption reactions are:

$$HA + > Ca^{2+} \underset{k-1}{\overset{k1}{\leftrightarrow}} HACa_{ads} \quad (3a)$$

and

$$CO_3^{2-} + > Ca^{2+} \underset{k-2}{\overset{k2}{\leftrightarrow}} CaCO_{3ads} \quad (3b)$$

If [Ca], [HA] and $[CO_3]$ are invariant at a fixed rate, the steady state equations are:

$$\frac{d[HACa]_{abs}}{dt} = 0 \quad (4a)$$

$$\frac{d[CaCO_3]_{abs}}{dt} = 0 \quad (4b)$$

Both Eqs. (4a) and (4b) can be solved for ϑ_{HA} and ϑ_{CO_3} using Eq. (1) (see Castellan, 1983). We will consider only the case for which k is very small (Brown et al., 1993). Assuming $k=0$, steady state equations are:

$$\vartheta_{HA} = K_1 \times [HA] \times \vartheta_v \quad (5a)$$

$$\vartheta_{CO_3} = K_2 \times [CO_3] \times \vartheta_v \quad (5b)$$

where

$$K_1 = k_1/k_{-1} \text{ and } K_2 = k_2/k_{-2} \quad \text{(reversibility of the reactions)} \quad (5c)$$

Substituting Eqs. (5a) and (5b) into Eq. (1) and rearranging we obtain:

$$\vartheta_v = \frac{1}{1 + K_1[HA] + K_2[CO_3]} \quad (6)$$

This value of ϑ_v brings Eqs. (5a) and (5b) to the form:

$$\vartheta_{HA} = \frac{K_1 \times [HA]}{1 + K_1 \times [HA] + K_2 \times [CO_3]} \quad (7a)$$

$$\vartheta_{CO_3} = \frac{K_2 \times [CO_3]}{1 + K_1 \times [HA] + K_2 \times [CO_3]} \quad (7b)$$

Substituting Eqs. (7a) and (7b) into Eq. (2) the rate law yields:

$$v = \frac{k \times K_1 \times K_2[> Ca] \times [HA] \times [CO_3]}{(1 + K_1 \times [HA] + K_2 \times [CO_3])^2} \quad (8)$$

The two limiting cases of Eq. (8) are:

1. If both HA and CO_3 are weakly adsorbed, the surface is sparsely covered. Under these conditions: $K_1 \times [HA] \ll 1$ and $K_2 \times [CO_3] \ll 1$. The denominator of Eq. (8) is about equal to unity and the rate law becomes:

   $$v = k \times K_1 \times K_2[> Ca] \times [HA] \times [CO_3] \quad (9)$$

   Under such a condition, the reaction of calcite crystal growth would increase by the presence of the DOM matter under the form of HA.
2. If HA is much more strongly adsorbed on the surface than CO_3: $K_1 \times [HA] \gg K_2 \times [CO_3]$ and $K_1 \times [HA] \gg 1$, and the rate equation becomes:

   $$v = \frac{k \times K_2 \times [Ca] \times [CO_3]}{K_1 \times [HA]} \quad (10)$$

   The rate of the reaction is inversely proportional to the concentration of the strongly adsorbed species and HA inhibits the reaction.

According to this highly simplified scenario, dissolved organic matter under the form of HA can enhance or limit the rate of calcite crystal growth depending on both concentration and adsorption constants clarifying the apparent contradiction between results of the different investigations (Suess, 1970; Berner et al., 1978; Wada et al., 1993). The results of this simplified model are in agreement with the high-resolution spectro-microscopic observations of Myneni et al. (1999). They found that HA exhibits more than one type of macromolecular structure at high ionic strength and weakly alkaline aqueous

solutions. The different organic groups thus behave differently with respect to their adsorption on carbonate surfaces. However, it still remains difficult to establish a rational predictive a priori model without a full determination of the HA microscopic properties at the seawater-solution carbonate interface.

3. Experimental

A slightly modified version of the constant addition technique (Zuddas and Mucci, 1994, 1998) was used to conduct the calcite crystal growth experiments. Initially proposed by Zhong and Mucci (1993), this experimental system provides a steady state environment during calcite growth and is suitable for investigations close to equilibrium conditions. This last condition, frequently found in natural solutions, is not easily simulated by experimental methods because of extremely slow reaction rates and presence of natural inhibitors (Morse and MacKenzie, 1990; Zhong and Mucci, 1993). The reactor consisted of a double-walled glass 500 ml separatory funnel in which the temperature of the precipitating solution was maintained at 298 ± 0.1 K by re-circulating water through the glass jacket from a constant temperature bath. A supersaturated solution (i.e. $1.2 < \Omega < 10$) was delivered to the reactor at a selected constant rate by a peristaltic pump using Tygon tubing. A water-saturated CO_2/N_2 gas mixture of known composition was introduced in the reactor, at a controlled rate, through a glass frit fitted at the bottom of the separatory funnel. Bubbling of the gas through the reacting solution served to maintain the P_{CO_2} at a desired and constant value, as well as keeping the mineral seed in suspension. The validity of the steady state operating assumption for the constant addition technique was theoretically and experimentally demonstrated by Zhong and Mucci (1993). In this work, it was confirmed by the constancy of pH and calcium concentration throughout the duration of the experiments.

3.1. Starting material

Baker 'Instra-analyzed flux reagent' grade calcite, treated by the procedure described by Mucci (1986) was used as seed material for the calcite precipitation experiments. Seeds have a well restricted size range between 3 and 7 μm as observed by Scanning Electron Microscopy (SEM) and a specific surface area respectively of 0.52 m^2/g as determined by the Kr-BET method (deKanel and Morse, 1979).

All experiments were performed in NaCl solutions at a total ionic strength of 0.7 mol/kg at a fixed calcium concentration of 0.01 mol/kg introduced as a chloride salt. Standard (Aldrich) humic acid (HA) was added at concentrations of 0.05, 0.5 and 1 mg/kg. To prevent microorganism development, solutions were prepared by deionised–bidistilled waters and $CdCl_2$ (i.e. 0.1–0.01 μmol/kg) was added. The functional groups of the HA standard were characterised following the method described by Stevenson (1982) and Alberti et al. (1994) and its composition is reported in Table 1. Solutions of a desired initial saturation state were obtained by adding appropriate amounts of Na_2CO_3 and $NaHCO_3$ to the $NaCl–CaCl_2$ solutions which had previously been equilibrated with a $CO_2–N_2$ gas mixture of known P_{CO_2}.

3.2. Experiments

The calcite crystal growth experiments were conducted by first introducing 0.1 to 0.4 g of carbonate seed into the empty reactor. The mineral growth was then initiated by pumping the supersaturated solution into the reactor at a constant rate. Typically, 6–8 ml of solution were sufficient to completely wet the solid. All the experiments were carried out at 298 ± 1 K and at a constant CO_2 partial pressure of 40 Pa. At the beginning, during, and at the end of each experiment, an aliquot of the reacting solution was sampled with a plastic syringe and canula, filtered through a Millipore® 0.45 μm filter, and stored in a plastic tube for later analysis. The pH of the reacting solution was monitored at regular intervals throughout the precip-

Table 1
Composition of the humic acid used in the experiments

Total acidity	5.43 meq/kg
Carboxylic groups	4.88 meq/g
Total C=O groups	1.97
Ketones groups	0.42
Quinine groups	1.55
Total OH-groups	2.27
Alcoholic OH groups	1.72
Phenol OH groups	0.55

itation using a combination glass-reference electrode and by the Zhong and Byrne (1996) colorimetric methods.

3.3. Analysis

Calcium concentration and carbonate alkalinity were determined by potentiometric titration according to procedures described by Mucci (1986). At high dissolved organic matter levels, calcium may be complexed by HA. Since the lack of quantitative model for strong electrolyte solutions (Tipping et al., 2002) a comparative titration (made with and without HA) indicates that the amount of complexed calcium is 25% and 10% when [HA] is 1000 and 100 μg/kg, respectively. At lower [HA], the binding HA action has been found to be negligible in our experimental conditions. Similarly, the negative charge of the HA in our experimental solutions has been estimated to correspond to 7% of the total alkalinity for the highest [HA].

The electrode used for pH potentiometric determination was calibrated against three NIST-traceable buffer solutions (pH = 4.01, 7.00, 9.00 at 298 K). Reproducibility of pH calibrations, carried out before and after measurements of a single solution, was better than 0.005 pH unit. Because of problems inherent to the use of glass electrodes calibrated using NIST buffers in strong electrolyte solutions (see DOE, 1994, for a review), this measurement was only used to verify that steady state conditions were maintained throughout the precipitation. Otherwise, pH was also measured by the colorimetric method of Zhong and Byrne (1996). Briefly, this methods is based on the proton exchange behaviour of thymol blue ($HI^- \leftrightarrow I^{2-} + H^+$) and the molar absorbance characteristic of the unprotonated (I^{2-}) and protonated (HI^-) forms of this indicator. The equation used to estimate pH in our strong electrolyte solution from spectrophotometric measurement was:

$$\mathrm{pH} = \mathrm{p}K_i + \log \frac{R - \frac{\varepsilon_{\mathrm{IH}}^{596}}{\varepsilon_{\mathrm{IH}}^{434}}}{\frac{\varepsilon_{\mathrm{I}}^{596}}{\varepsilon_{\mathrm{IH}}^{434}} - R \times \frac{\varepsilon_{\mathrm{I}}^{434}}{\varepsilon_{\mathrm{IH}}^{434}}} \quad (11)$$

where pK_i is equal to 8.559, R is the ratio of the absorbencies produced by thymol blue in our experimental solutions at the absorbance maxima of I^{2-} (596 nm) and HI^- (434 nm), and ε_x^{λ} is the molar absorption coefficient of I^{2-} (or HI^-) at wavelength λ (Lefèvre et al., 1993; Zhong and Byrne, 1996).

Morphologies of reacted and unreacted calcite crystals were examined using the JEOL Scanning Electron Microscopy (SEM).

3.4. Aqueous solution calculations

The saturation state of the precipitating solution with respect to calcite, Ω_c, was calculated according to:

$$\Omega_c = [Ca^{2+}][CO_3^{2-}]/K_C^* \quad (12)$$

where K_C^* is the calcite stoichiometric solubility constant in the $NaCl–CaCl_2$ solutions.

The total calcium concentration was measured directly, while the CO_3^{2-} ion concentration was calculated from pH, carbonate alkalinity and appropriate stoichiometric equilibrium constants of the carbonic acid system.

The CO_2 solubility, carbonic acid stoichiometric dissociation and calcite solubility constants in our experimental solutions were calculated from constants determined in seawater $K_{i(sw)}^*$ at equivalent ionic strengths (Weiss, 1974; Mucci, 1983; Roy et al., 1993) and total ion activity coefficients γ_i of the carbonic acid species in the experimental solution. The ion pairing model of Millero and Scheiber (1982) was used to estimate the ion activity coefficients, $\gamma_{i,}$ at each ionic strength.

$$K_{1(\mathrm{NaCl})}^* = K_{1(\mathrm{sw})}^* \frac{\gamma_{\mathrm{HCO_3(sw)}}}{\gamma_{\mathrm{HCO_{3(NaCl)}}}} \quad (13)$$

$$K_{2(\mathrm{NaCl})}^* = K_{2(\mathrm{sw})}^* \frac{\gamma_{\mathrm{CO_{3(sw)}}}\gamma_{\mathrm{HCO_{3(NaCl)}}}}{\gamma_{\mathrm{CO_{3(NaCl)}}}\gamma_{\mathrm{HCO_{3(sw)}}}} \quad (14)$$

$$K_{c(\mathrm{NaCl})}^* = K_{c(\mathrm{sw})}^* \frac{\gamma_{\mathrm{Ca(sw)}}\gamma_{\mathrm{CO_{3(sw)}}}}{\gamma_{\mathrm{Ca(NaCl)}}\gamma_{\mathrm{CO_{3(NaCl)}}}} \quad (15)$$

The estimated calcite stoichiometric solubility constants and carbonic acid dissociation constants are reported in Table 2. The uncertainty on the carbonate ion speciation is estimated to be between 8% and 10% of the $Log[CO_3^{2-}]$ values.

Table 2
Apparent dissociation constants of carbonic acid and stoichiometric solubility of calcite in NaCl–$CaCl_2$ solutions at the ionic strength of 0.7 mol/kg (T=298.15 K, P_{CO_2}=40 Pa)

$\alpha=[H_2CO_3]/P_{CO_2}=0.0028$
$K_1'=10^{-pH}\times[HCO_3^-]/[H_2CO_3]=9.72\times10^{-7}$
$K_2'=10^{-pH}\times[CO_3^{2-}]/[HCO_3^-]=4.68\times10^{-10}$
$K_c'=[Ca^{2+}]\times[CO_3^{2-}]=2.29\times10^{-7}$

Table 3
Least-squares fit parameter to the empirical rate model for calcite crystal growth

HA	n	Log k	r
0	1.41 ± 0.31	2.18 ± 0.21	0.88
50	1.22 ± 0.31	1.82 ± 0.15	0.75
500	1.46 ± 0.41	1.24 ± 0.15	0.92
1000	2.10 ± 0.51	0.19 ± 0.21	0.92

3.5. Rate estimation

The precipitation rate (R, μmol m^{-2} h^{-1}) was calculated from the difference in carbonate alkalinity (meq/kg) between the input (Alk_0) and reacting (Alk_{ss}) solutions at steady state and i, the injection rate (kg h^{-1}). The rate was normalized to the initial surface area of the calcite seeds:

$$R = i(\mathrm{Alk}_0 - \mathrm{Alk}_{SS})/SW_{seed} \quad (16)$$

where W_{seed} is the initial weight of the calcite seed and S is the specific reactive surface area. Since less than 10% of the initial seed weight was precipitated during any given experiment, surface area variations were neglected in the rate calculations. The uncertainty on these rate measurements is estimated to be between 3% and 8% of the log R values.

4. Results

Classically, mineral precipitation and dissolution rates have most often been expressed in terms of a functional dependence. Similarly, in seawater solutions and other strong electrolyte solutions, precipitation rate data of calcite have commonly been fitted to an empirical rate law of the following canonic form (Nancollas and Reddy, 1971; Morse, 1978; Berner and Morse, 1974; Reddy and Gaillard, 1981):

$$R = k(\Omega - 1)^n \quad (17)$$

or in its logarithmic form:

$$\log R = n\log(\Omega - 1) + \log k \quad (18)$$

where R is the measured reaction rate, k is the rate constant, and n is the empirical global reaction order.

This empirical rate law fits our data very well over the whole range of supersaturation and dissolved organic matter concentrations covered in this study (Table 3; Fig. 1). This fit was derived by a least-square calculation (Brooks et al., 1972) and the errors propagated according to the Minster et al. (1979) and Provost (1990) procedures. The data obtained at different HA content, however, do not plot on the same line, and yield distinct kinetic parameters. Over the range of HA investigated, the empirical reaction order remains constant while the rate constant decreases as the HA increases (Table 3). Previous experimental investigations carried out in artificial seawater solutions have demonstrated that when fitted to the same expression, the rate of carbonate crystal growth is inhibited by the presence of dissolved organic matter (Suess, 1970; Berner et al., 1978). Our kinetic data extend the validity of this conclusion to calcite in NaCl–$CaCl_2$ solutions. This empirical

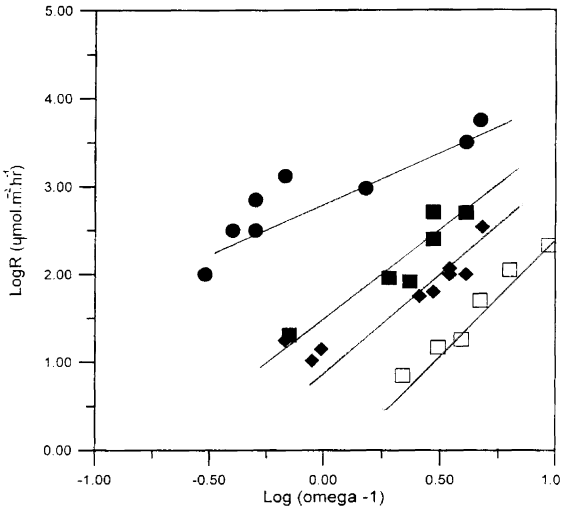

Fig. 1. Log R (rate) as a function of Log ($\Omega - 1$) for calcite in 0.7 m NaCl–$CaCl_2$ solutions at 298.15 K and various [HA]. Circles at [HA]=0; solid squares at [HA]=50 μg/kg; rhombs at [HA]=500 μg/kg; open squares at 1000 μg/kg.

approach however does not allow any insight as to how the growth is affected by the presence of dissolved organic matter in parent solutions.

In seawater solutions, as well in strong electrolyte solutions of similar ionic strength (i.e. 0.7 M), the rate at 298 K and over a range of P_{CO_2} between 10 and 10^3 Pa, is controlled by the reaction (Zhong and Mucci, 1993; Zuddas and Mucci, 1994):

$$Ca^{2+} + CO_3^{2-} \underset{k_b}{\overset{k_f}{\leftrightarrow}} CaCO_3 \quad (19)$$

The net experimental rate R, being the difference between the precipitation rate R_f, and the dissolution rate R_b can be written as:

$$R = R_f - R_b = k_f(a_{Ca^{2+}})^{n_1}(a_{CO_3^{2-}})^{n_2} - k_b(a_{CaCO_3})^{n_3} \quad (20)$$

where k_f and k_b are the forward and reverse reaction rate constants, a_i and n_i are, respectively, the activities and partial reaction orders for the species involved. Assuming that the activity of a relatively pure solid is unity, Eq. (20) can be reduced to:

$$R = k_f(a_{Ca^{2+}})^{n_1}(a_{CO_3^{2-}})^{n_2} - k_b \quad (21)$$

Precipitation rates are, a priori, highly dependent on the a_{Ca}/a_{CO_3} ratio of the solution (Winter and Burton, 1992) and rate expressions based solely on carbonate species or on the ion activity product do not accurately predict precipitation rate dependence. However, in solutions where the concentration of calcium ions is nearly constant and much larger than that of carbonate ions, Zuddas and Mucci (1998) demonstrated that the kinetics of calcite precipitation can be described considering $[CO_3^{2-}]$ as a sole or governing variable and that the rate of calcite crystal growth is pseudo-zero order with respect to the $[Ca^{2+}]$. Eq. (21) can then be reduced to:

$$R = K_f[CO_3^{2-}]^{n_2} - k_b \quad (22)$$

where

$$K_f = k_f(\gamma_{CO_3^{2-}})^{n_2}(a_{Ca^{2+}})^{n_1} \quad (22a)$$

is a constant for a given solution composition (i.e, I, Ω_c).

Eq. (22) can also be written in the logarithmic form:

$$\log(R + k_b) = n_2 \log[CO_3^{2-}] + \log K_f \quad (23)$$

The parameterisation of the kinetic model expressed by Eq. (23) depends mainly on the estimation of the carbonate ion concentrations. The rate data obtained at each of the HA concentration investigated in this study were fitted to Eq. (23) (Fig. 2) for log $[CO_3^{2-}] > -1.45$ ($\Omega > 2$; $k_b \rightarrow 0$). The least-squares fit parameters corresponding to the partial reaction order of the carbonate ion (n_2, slope) and apparent forward rate constant (K_f, intercept) are reported in Table 4 for each HA concentration. The data obtained in this study show that the partial reaction order with respect to the carbonate ion concentration remains equal to 3. Thus, it would appear that the mechanism of calcite growth is not significantly influenced by the presence of dissolved organic matter at this scale of measurements. However, the apparent forward rate constant decreases by one order of magnitude in the presence of HA showing an inhibition induced by the presence of HA and indicating that HA are more strongly

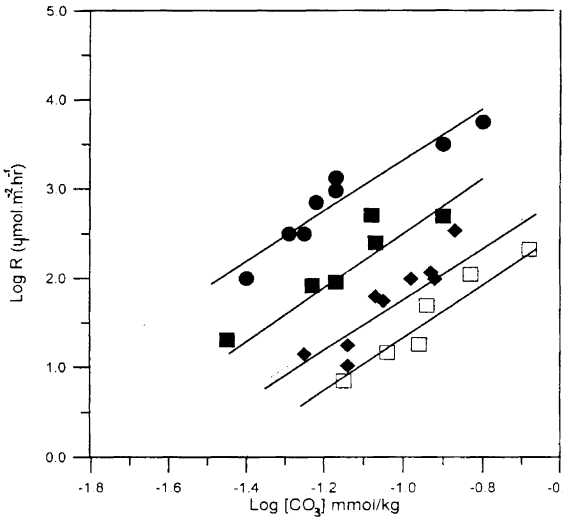

Fig. 2. Log R (rate) as a function of log (CO_3^{2-}) for calcite in 0.7 m $NaCl-CaCl_2$ solutions at 298.15 K and various [HA]. Circles at [HA] = 0; solid squares at [HA] = 50 μg/kg; rhombs at [HA] = 500 μg/kg; open squares at [HA] = 1000 μg/kg.

Table 4
Least-square fit kinetic parameter evaluated from rate measurements conducted far from equilibrium conditions (Ω>1.6) for calcite crystal growth experiments

HA	n_2	Log K_f	r
0	2.80 ± 0.45	5.80 ± 0.47	0.95
50	2.80 ± 0.47	5.26 ± 0.50	0.85
500	3.00 ± 0.50	5.00 ± 0.48	0.92
1000	3.18 ± 0.47	4.76. ± 0.47	0.95

adsorbed on the calcite surface than CO_3 ions. Examining the morphological changes that occurred during growth with and without added HA, we found that while unreacted crystals were well formed, sharp-edged rhombohedra bounded by $(10\bar{1}4)$ faces, crystals that grew in the absence of HA exhibited smooth planes of growth with steps of relatively uniform thickness (Fig. 3A). In contrast, the morphology of the crystals produced by growth in the presence of HA (0.5 mg/kg) and for which the growth rate was reduced by one order of magnitude, exhibited planes on which growth had been interrupted, resulting in a broken or discontinuous appearance (Fig. 3B and C). Dissolved organic matter in the form of HA thus inhibits the rate of calcite crystal growth in strong electrolyte solutions of ionic strength like seawater by blocking the active growth sites.

To estimate the influence of [HA] on the kinetics of calcite precipitation from seawater solutions, we relate the effect of the dissolved HA observed in this study to that generated by other inorganic seawater constituents such as Mg^{2+} and SO_4^{2-}, which inhibit calcite precipitation (Reddy and Wang, 1980; Reddy, 1995) and are responsible for 20–30-fold decrease in the precipitation/growth rate (Zuddas and Mucci, 1994). Using the classical kinetic formalism (Lasaga, 1998), the rate of calcite crystal growth from seawater at constant temperature and ionic strength can be expressed by the following general equation:

$$R = k_0 g(P_{CO_2}) \Pi a_i f(\Delta G) \quad (24)$$

where k_0 is the kinetic constant, $g(P_{CO_2})$ is the dependence on the P_{CO_2} partial pressure at equilibrium with the solution, Πa_i is the product of the activity of the inorganic and organic inhibitors of the reaction, and $f(\Delta G)$ introduces the supersaturation state of the solution expressed as a function, f, of the free-energy change ΔG.

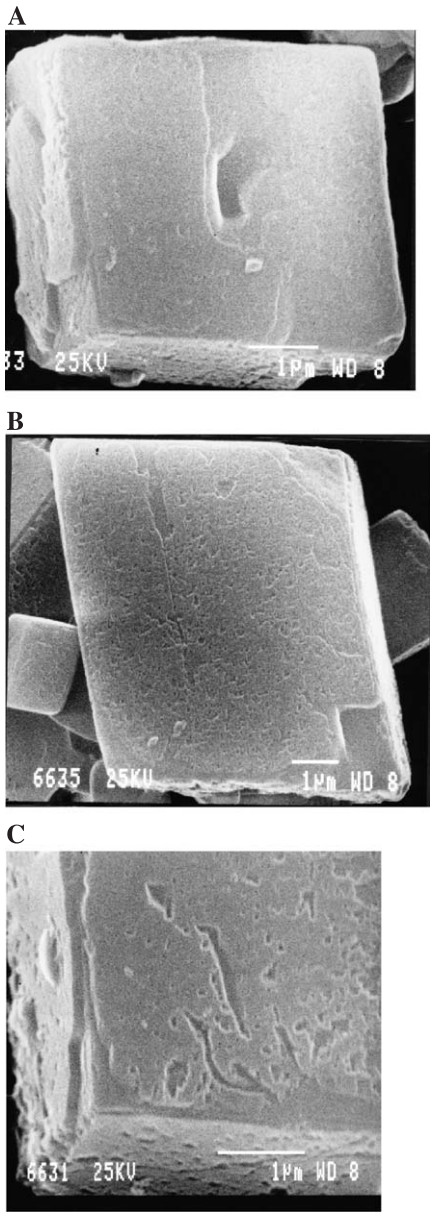

Fig. 3. SEM photomicrographs of calcite seed material after crystal growth experiments. Calcite seed in experiments with no added HA (A) where a lateral continuous plane of growth can be observed. Calcite seed after growing in solution containing 50 (B) and 500 (C) μg/kg HA where laterally discontinuous planes of growth are observed.

Assuming $f(\Delta G) = \Delta G/RT$, where R is the gas constant and T the absolute temperature (Lasaga, 1998), Eq. (24) can be parameterised using the data on the catalytic effect of P_{CO_2} partial pressure reported by Zuddas and Mucci (1994) and the inhibition of the inorganic seawater constituents (Zhong and Mucci, 1993):

$$\log \text{Rate} = 9.6 + 0.33 \times \log P_{CO_2} - \log[\text{HA}] + 3 \times \log[CO_3] \quad (24a)$$

with: $30 < P_{CO_2} < 10^4$ Pa; and $1 < [\text{HA}] < 10^3$ μg/kg.

Eq. (24a) indicates that, when the carbonate ion concentration is between 0.01 and 0.1 mmol/kg at the ionic strength of 0.7 mol/kg and the P_{CO_2} partial pressure is between 40 and 100 Pa (neritic and diagenetic seawater conditions), the rate of calcite precipitation from seawater decreases by one order of magnitude as a result of a 1000-fold increase in the HA concentration of the parent solution.

5. Discussion and conclusions

Given its different behaviour in strong electrolyte and weakly alkaline aqueous solutions, dissolved organic matter under the form of humic acid may limit or enhance the rate of calcite crystal growth depending on both concentration and adsorption constants. Experiments carried out in $NaCl-CaCl_2$ solutions of similar ionic strength as seawater (i.e. 0.7 mol/kg) indicate that while the partial reaction order with respect to the $[CO_3^{2-}]$ concentration remains unchanged, the reaction rate decreases by one order of magnitude as the [HA] increases from 0 to 1000 μg/kg. In addition to a decrease of the rate constant, we propose that the inhibition of calcite crystal growth results from a decrease of active growth sites rather than a decrease in the amount of free-calcium resulting from complexation with HA. These results contrast with the conclusion of previous studies in which rate data were fitted to a single empirical model and on the basis of which it was suggested that dissolved organic matter complexing free-calcium ions reduces the saturation state of the solution and consequently decreases the reaction rate.

Relating the observed effects of the dissolved HA found in this study to that generated by other inorganic seawater constituents, especially sulphate and magnesium (Zhong and Mucci, 1993; Zuddas and Mucci, 1994), our model shows that the precipitation rate still decreases by one order of magnitude as a result of the three-fold increase of the [HA] of the solution. However, the surface roughness that developed during calcite growth from solutions containing high HA concentrations results in an increase of the reactive surface area and may had to an underestimation of this inhibition effect. Semi-quantitatively, comparing the total number of surface sites available in 0.1 mg of calcite seed to the amount of HA in solution (assuming a molecular weight of 1200) and assuming 5 sites/nm^2 on the calcite surface (Davis and Kent, 1990), the available sites would be about 10^{14}, while the number of molecules of organic acid in the experiments would be 0.4×10^{13}. This may indicate that the growth inhibition is governed by large organic molecules able to adsorb to more than one growth site on the calcite surface. Our results are in agreement with Mayer (1994) and Troy et al. (1997) observations on calcareous particles on shelf regions, where it was found that an incorporation of high levels of organic carbon in surface pore produces an increases of the surface area of at least two orders of magnitude. More careful assessment on the spatial relationship between organic matter (i.e. adsorption) and micro-topography is, however, necessary to establish the quantitative role of ‘geo-polymer’ such as HA with calcium carbonate surface under seawater solution conditions.

Acknowledgements

We acknowledge Dr. J.P. Ciabrini who introduced us to pH spectrometric measurements, Dr. A. Cristini and Dr. G. Alberti for the Humic Acid analysis and Dr. P. Blanc for technical assistance in SEM observations. The authors appreciate the careful reviews by Dr. A. Mucci and two anonymous C.G. reviewers that improved the quality of the manuscript. Financial support was provided by IPGP-BQR1998 grant. **[CA]**

Appendix A

Data for crystal growth rates in $NaCl_2$ solutions at $I = 0.7$ mol/kg for different [HA].

Log R, μmol m^{-2} h^{-1}	Alc_{tot}, mmol/kg	pH	Humic acid, μg/kg
3.12	2.35	7.81	0
2.85	0.65	7.80	
2.5	0.67	7.91	
3.75	2.92	8.10	
2.98	2.26	7.76	
2.5	0.68	7.94	
3.5	2.39	8.03	
2.00	0.60	7.90	
2.71	2.05	7.98	50
2.40	2.04	7.98	
1.92	2.91	7.77	
1.96	2.50	7.74	
1.31	2.38	7.68	
2.70	2.39	8.05	
2.00	2.25	8.03	500
1.80	2.05	7.98	
1.15	1.42	7.85	
2.00	2.39	8.05	
1.75	1.98	8.00	
1.02	2.53	7.80	
2.07	2.67	8.02	
2.54	2.72	8.08	
1.25	2.38	7.75	
2.33	3.57	8.15	1000
2.05	2.69	8.12	
1.07	2.18	8.10	
1.26	2.56	8.00	
1.17	2.37	7.95	
0.85	0.30	8.05	

References

Alberti, G., Cabiddu, S., Cristini, A., Loi, A., Sotgiu, F., 1994. Heavy metal–humic acid interaction in environments of Southern Sardinia. In: Senesi, N., Miano, T.M. (Eds.), Humic Substance in the Global Environment and Implication on Human Health. Elsevier, pp. 1073–1078.

Berner, R.A., Morse, J.W., 1974. Dissolution kinetics of calcium carbonate in seawater: IV. Theory of calcite dissolution. Am. J. Sci. 274, 108–135.

Berner, R.A., Westrich, J.T., Graber, R., Smith, J., Martens, C.S., 1978. Inhibition of aragonite precipitation from supersaturated seawater. A laboratory and field study. Am. J. Sci. 278, 816–837.

Bischoff, J.L., 1968. Catalysis, inhibition, and the calcite aragonite problem. Am. J. Sci. 266, 80–90.

Brooks, C., Hart, S.R., Wendt, I., 1972. Realistic use of two errors regression treatments as applied to rubidium–strontium data. Rev. Geophys. Space Phys. 10, 551–577.

Brown, C.A., Compton, R.G., Narramore, C., 1993. The kinetics of calcite dissolution–precipitation. J. Colloid Interface Sci. 160, 372–379.

Burton, E.A., Walter, L.M., 1987. Relative precipitation rates of aragonites and Mg calcite from seawater: temperature or carbonate ion control? Geology 15, 111–114.

Castellan, G.W., 1983. Physical Chemistry. Benjamin Cummings, Menlo Park.

Chave, K., Suess, E., 1970. Calcium carbonate saturation in seawater: effect of dissolved organic matter. Limnol. Oceanogr. 15, 633–637.

Cicerone, D.S., Regazzoni, A.E., Blesa, M.A., 1992. Electrokinetic properties of the calcite/water interface in the presence of magnesium and organic matter. J. Colloid Interface Sci. 154, 423–433.

Davis, J.A., Kent, D.B., 1990. Surface complex modelling in geochemistry. In: Hochella, M.F., White, A.F. (Eds.), Mineral–Water Interface Geochemistry. Mineralogical Society of America, pp. 177–260.

DeKanel, J., Morse, J.W., 1979. A simple technique for surface area determinations. J. Phys. E: Sci. Instrum. 12, 272–273.

DOE, 1994. In: Dickson, A.G., Goyet, C. (Eds.), Handbook of Methods for the Analysis of the Various Parameters of the Carbon Dioxide System in Seawaters. Version 2. ORNL-CDIAC-74.

Kitano, Y., Hood, D.W., 1965. The influence of organic material on the polymorphic crystallisation of calcium carbonate. Geochim. Cosmochim. Acta 29, 29–41.

Kitano, Y., Kanamori, N., 1966. Synthesis of magnesium calcite at low temperatures and pressures. J. Geochem. 1, 1–11.

Lasaga, A., 1998. Kinetic Theory in the Earth Sciences. Princeton Series in Geochemistry. 811 pp.

Lefèvre, N., Ciabrini, J.P., Michard, G., Brient, B., Duchafaut, M., Merlivat, L., 1993. A new optical sensor for P_{CO_2} measurements in seawater. Mar. Chem. 42, 189–198.

Mayer, L.M., 1994. Surface area control of organic carbon accumulation in continental shelf sediments. Geochim. Cosmochim. Acta 58 (4), 1271–1284.

Millero, F.J., Scheiber, D.R., 1982. Use of the ion pairing model to estimate activity coefficients of the ionic components of natural water. Am. J. Sci. 282, 1508–1540.

Minster, J.F., Ricard, L.P., Allègre, C.J., 1979. ^{87}Rb–^{87}Sr chronology of enstatite meteorites. Earth Planet. Sci. Lett. 44, 420–440.

Morse, J.W., 1978. Dissolution kinetics of calcium carbonate in seawater: VI. The near-equilibrium dissolution kinetics of calcium carbonate-rich deep sea sediments. Am. J. Sci. 278, 344–355.

Morse, J.W., Mackenzie, F.T., 1990. Geochemistry of Sedimentary Carbonates. Elsevier, New York. 707 pp.

Mucci, A., 1983. The solubility of calcite and aragonite in seawater at various salinities, temperatures, and one atmosphere total pressure. Am. J. Sci. 283, 780–799.

Mucci, A., 1986. Growth kinetics and composition of magnesian calcite overgrowths precipitated from seawater: quantitative influence of orthophosphate ions. Geochim. Cosmochim. Acta 50, 2255–2265.

Myneni, S.C.B., Brown, J.T., Martinez, G.A., Meyer-Ilse, W., 1999. Imaging humic substance macromolecular structures in water and soils. Science 286, 1335–1337.

Nancollas, G.H., Reddy, M.M., 1971. The crystallisation of calcium carbonate: II. Calcite growth mechanism. J. Colloid Interface Sci. 37, 824–830.

Plummer, L.N., Wigley, T.M.L., Parthurst, D.L., 1978. The kinetics of calcite dissolution in CO_2–water system at 5° to 60 °C and 0.0 to 1.0 atm. CO_2. Am. J. Sci. 278, 179–216.

Provost, A., 1990. An improved diagram for isochron data. Chem. Geol., Isot. Geosci. Sect. 80, 85–99.

Reddy, M.M., 1995. Calcite precipitation in Pyramid lake, Nevada. In: Zahid, A. (Ed.), Mineral Scale Formation and Inhibition. Plenum, pp. 21–31.

Reddy, M.M., Gaillard, W.D., 1981. Kinetics of calcium carbonate (calcite) seeded crystallization: influence of solid/solution ratio on the reaction rate constant. J. Colloid Interface Sci. 80, 171–178.

Reddy, M.M., Wang, K.K., 1980. Crystallisation of calcium carbonate in the presence of metal ions: I. Inhibition by magnesium ions at pH 8.8 and 25 °C. J. Cryst. Growth 50, 470–480.

Roy, R.N., Roy, L.N., Vogel, K.M., Porter-Moore, C., Pearson, T., Good, C., Millero, F., Campbell, D., 1993. The dissociation constants of carbonic acid in seawater at salinities 5 to 45 and temperatures 0 to 45 °C. Mar. Chem. 44, 249–267.

Stevenson, F.J., 1982. Humus Chemistry, Genesis, Composition, Reactions. Wiley, New York.

Suess, E., 1970. Interaction of organic compounds with calcium carbonate: I. Association phenomena and implications. Geochim. Cosmochim. Acta 34, 157–168.

Tipping, E., Rey-Castro, C., Bryan, S., Hamilton-Taylor, J., 2002. Al(III) and Fe(III) binding humic substances in freshwaters, and implication for trace metal speciation. Geochem. Cosmochim. Acta 66 (18), 3211–3224.

Troy, P.J., Yuan-Hui, L., MacKenzie, F.T., 1997. Changes in surface morphology of calcite exposed to the oceanic water column. Aquat. Geochem. 3, 1–20.

Wada, N., Okazaki, M., Tachikawa, S., 1993. Effects of calcium-binding polysaccharides from calcareous algae on calcium carbonate polymorphs under conditions of double diffusion. J. Cryst. Growth 132, 115–121.

Winter, D.J., Burton, E.A., 1992. Experimental investigation of a_{Ca}/a_{CO_3} ratio on the kinetics of calcite precipitation: implication for the rate equation and trace element incorporation. Geol. Soc. Amer. Ann. Meeting, A37 (abstract).

Weiss, R., 1974. Carbon dioxide in water and seawater. The solubility of a non-ideal gas. Mar. Chem. 2, 203–215.

Zhong, H., Byrne, R.H., 1996. Spectrophotometric pH measurements of surface seawater at in-situ conditions: absorbance and protonation behavior of thymol blue. Mar. Chem. 52, 17–25.

Zhong, S., Mucci, A., 1993. Calcite precipitation in seawater using a constant addition technique: a new overall reaction kinetic expression. Geochim. Cosmochim. Acta 57, 1409–1417.

Zuddas, P., Mucci, A., 1994. Kinetics of calcite precipitation from seawater: I. A classic chemical kinetics description for strong electrolyte solutions. Geochim. Cosmochim. Acta 58, 4353–4362.

Zuddas, P., Mucci, A., 1998. Kinetics of calcite precipitation from seawater: II. The influence of the ionic strength. Geochem. Cosmochim. Acta 62 (5), 757–766.

View publication stats